

Christophe Wirth,[‡] Françoise Hoegy, Franc Pattus and David Cobessi*

Institut Gilbert-Laustriat UMR 7175 CNRS/
Université Strasbourg I, Département Récepteurs
et Protéines Membranaires, Ecole Supérieure de
Biotechnologie de Strasbourg, Boulevard
Sébastien Brandt, BP 10413, F-67412 Illkirch,
France

[‡] Present address: Department of Structural
Biology, Biozentrum, University of Basel,
Klingelbergstrasse 50/70, CH-4056 Basel,
Switzerland.

Correspondence e-mail:
cobessi@esbs.u-strasbg.fr

Received 14 February 2006
Accepted 6 April 2006

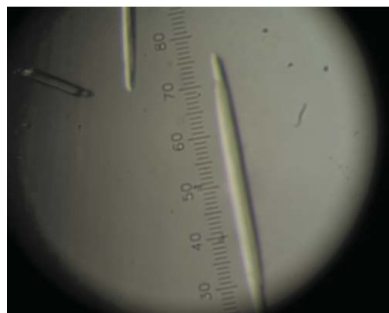
Preliminary X-ray investigations of several crystal forms of the ferripyoverdine FpvA outer membrane receptor from *Pseudomonas aeruginosa* bound to ferripyoverdine

Ferripyoverdine transport across the outer membrane of *Pseudomonas aeruginosa* by the pyoverdine receptor FpvA and the transcriptional regulation of FpvA involve interactions of the FpvA N-terminal TonB box and signalling domain with proteins from the inner membrane. Several crystallization conditions of FpvA–Pvd–Fe solubilized in C₈E₄ detergent were obtained and X-ray data were collected from three crystal forms. The resolution limits range from 3.15 to 2.7 Å depending on the crystal form. From preliminary analysis of the electron-density maps, the first full-length structure of an outer membrane receptor including a signalling domain should be determined.

1. Introduction

When grown under iron-deficient conditions, many bacteria synthesize and release into the environment iron chelators termed siderophores. These small molecules (MW 350–1500 Da) compete with host iron-storage proteins for iron. The iron-siderophores and other molecules larger than 600 Da such as vitamin B₁₂ do not passively diffuse through the outer membrane *via* porins or substrate-specific porins, but are instead transported by TonB-dependent receptors (TBDRs; Ferguson & Deisenhofer, 2002, 2004). The transport into the periplasm requires the proton motive force and the energy-transduction complex TonB–ExbB–ExbD of the cytoplasmic membrane (Ferguson & Deisenhofer, 2002, 2004). On the basis of their sequences, the TBDRs can be divided into four classes: the conventional TonB-dependent receptors (1) and transducers (2) and the Oar subclass TonB-dependent transducers (3) and receptors (4) (Koebnik, 2005). One of these classes includes TBDRs with a signalling domain upstream of the TonB box which interacts with a sigma regulator of the inner membrane. This inner membrane protein interacts with a cytoplasmic sigma-factor protein. The receptors of this class are called outer membrane transducers and are able to down-regulate their own synthesis as well as that of their cognate siderophore by binding the ferric siderophore (Braun *et al.*, 2003; Schalk *et al.*, 2004). To date, only the three-dimensional structure of the outer-membrane transducers FecA from *Escherichia coli* (Ferguson & Deisenhofer, 2002; Yue *et al.*, 2003) and FpvA from *Pseudomonas aeruginosa* (Cobessi *et al.*, 2005) have been solved, but their structural studies did not reveal the structure of the signalling domain. The structure of the FecA signalling domain was recently solved by NMR (Garcia-Herrero & Vogel, 2005).

P. aeruginosa is an opportunistic human pathogen which infects injured, immunodeficient or otherwise compromised patients. Under iron-limited conditions, the bacterium secretes a major siderophore: pyoverdine (Pvd; Poole & McKay, 2003). Pvd seems to play an important role in infection by competing with transferrin for iron in order to overcome the iron-withholding mechanism present in mammals. Because of the importance of *P. aeruginosa* in human infections and its growing resistance to antibiotics, we undertook crystallographic studies of the pyoverdine outer membrane receptor FpvA of *P. aeruginosa* bound to ferripyoverdine (FpvA–Pvd–Fe). Here, we describe the crystallization conditions and preliminary data analysis of FpvA–Pvd–Fe in several crystal packings which should provide structural information about the signalling domain.



2. Materials and methods

2.1. Expression and purification

FpvA (MW 86 469 Da) was expressed from the pyoverdine-deficient strain CDC5 transformed with the pPVR2 plasmid carrying the *fpva* gene (Poole *et al.*, 1993) and purified as described in Schalk *et al.* (1999). This strain, which is unable to synthesize Pvd, overproduces FpvA when grown in succinate medium (Demange *et al.*, 1990). However, by monitoring the fluorescence resonance energy transfer (FRET) from the tryptophans (Schalk *et al.*, 1999), we could still detect a small signal from a fluorescent molecule, which was likely to be a Pvd precursor bound in the Pvd-binding site. At the end of the purification, detergent exchange was performed by ultrafiltration at 3500g using a 30 kDa molecular-weight cutoff membrane (Amicon, Millipore). FpvA was mixed with Pvd-Fe or Pvd-Ga in a 100-fold excess and stored for 72 h at 277 K in order to totally substitute the fluorescent molecule from FpvA in 10 mM Tris-HCl pH 8.0 buffer containing 150 mM NaCl and 0.6% octyl-POE. The Pvd-Fe/Ga excess was removed by ultrafiltration. The total incorporation of Pvd-Fe was verified by the absence of FRET signal (Schalk *et al.*, 1999) (Fig. 1). Detergent exchange from octyl-POE to 0.5% (v/v) C₈E₄ was performed prior to the crystallization experiments.

2.2. Crystallization

Initial screenings were conducted at 293 K using the sitting-drop vapour-diffusion method and the sparse-matrix sampling approach (Jancarik & Kim, 1991; Cudney *et al.*, 1994) with the Classical Lite sparse matrix from Nextal. The reservoir volume was 80 μ l. 0.5 μ l protein solution was mixed with an equal volume of reservoir solution. The protein concentrations range from 5 to 15 mg ml⁻¹. Several crystallization conditions were found. Three crystallization conditions were refined using the sitting-drop vapour-diffusion method in Limbro plates by mixing 0.5 or 1 μ l protein solution with an equal volume of reservoir solution and equilibrating against the same precipitant. In this case, the reservoir volume was 500 μ l.

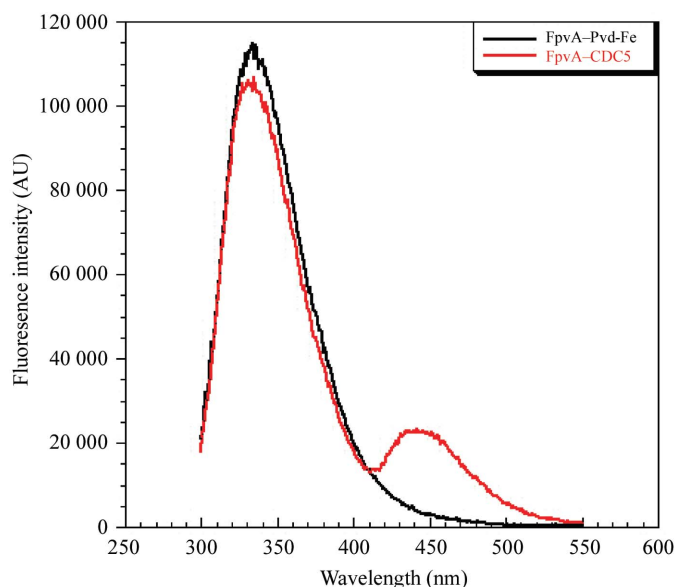
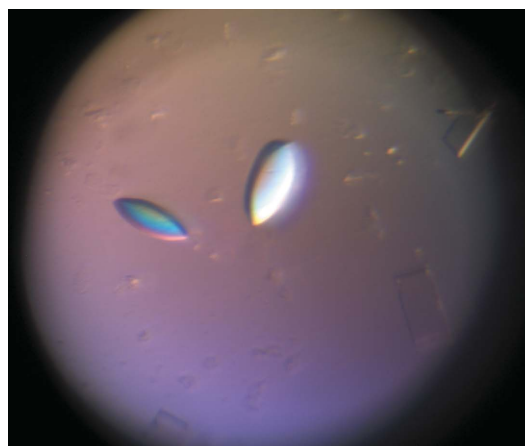


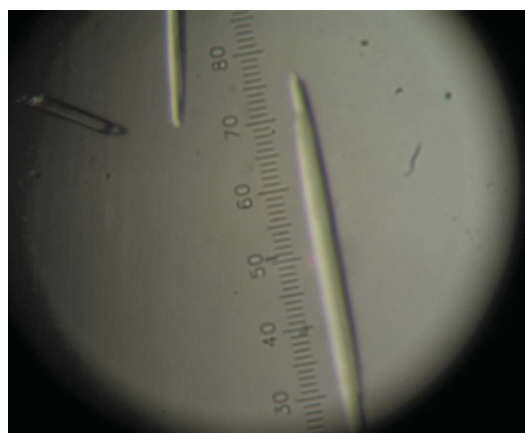
Figure 1 Fluorescence spectra of FpvA purified from strain CDC5 (red line) and of FpvA-Pvd-Fe (black line). The emission at 447 nm is absent in FpvA-Pvd-Fe, resulting from the binding of Pvd-Fe to FpvA purified from the strain CDC5. The excitation wavelength was set at 290 nm. Proteins were in 10 mM Tris-HCl pH 8.0, 150 mM NaCl and 0.6% octyl-POE.

2.3. Data collection and processing

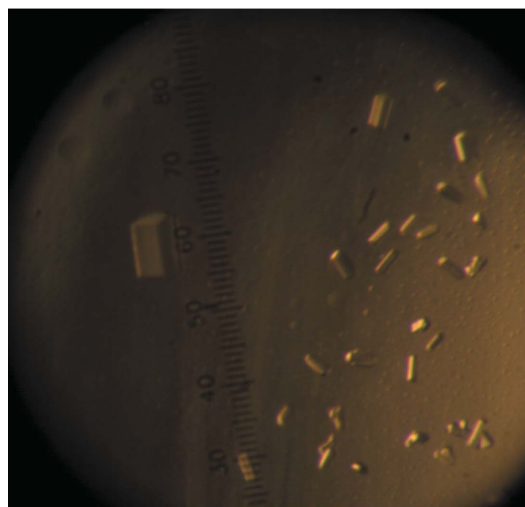
X-ray diffraction experiments were performed at 100 K on crystals mounted in cryoloops and flash-frozen in liquid nitrogen. X-ray data for the first crystal form were collected on beamline ID29 at ESRF at 100 K. Prior to data collection, crystals were soaked in crystallization



(a)



(b)



(c)

Figure 2 Pictures of the three FpvA-Pvd-Fe crystal forms. (a) Form 1: the crystals reach typical dimensions of 0.125 mm radius and 0.05 mm width. (b) Form 2: the crystals reach typical dimensions of 1.0 \times 0.12 \times 0.12 mm. (c) Form 3: the crystals reach typical dimensions of 0.2 \times 0.2 \times 0.1 mm.

Table 1

X-ray data statistics.

Values indicated in parentheses are for the highest resolution shell.

| Crystal form | Form 1 | Form 2 | Form 3 |
|--------------------------------|------------------------------|---|---|
| Wavelength (Å) | 0.97857 | 0.979751 | 1.0026 |
| Resolution (Å) | 46.9–2.73 (2.88–2.73) | 19.99–2.70 (2.75–2.70) | 19.97–3.15 (3.20–3.15) |
| Space group | $P4_12_12$ | $C2$ | $C2$ |
| Unit-cell parameters (Å, °) | $a = 82.12,$ $c = 286.23$ | $a = 140.09,$ $b = 235.03,$ $c = 237.25,$ $\beta = 101.12$ | $a = 174.11,$ $b = 123.13,$ $c = 118.30,$ $\beta = 121.49$ |
| Total reflections | 73207 (6431) | 639603 (17322) | 155299 (7159) |
| Unique reflections | 25462 (2982) | 194355 (8565) | 36743 (1671) |
| Completeness (%) | 94.4 (78.3) | 94.5 (78.1) | 99.2 (99.9) |
| $I/\sigma(I)$ | 7.3 (1.3) | 7.14 (1.52) | 9.48 (2.34) |
| R_{sym}^\dagger (%) | 4.5 (27.4) | 14.3 (54.9) | 16.6 (70.2) |

$^\dagger R_{\text{sym}} = \sum \sum |I_i - I_m| / \sum \sum I_i$, where I_i is the intensity of the measured reflection and I_m is the mean intensity of this reflection.

solution containing 30% ethylene glycol as a cryoprotecting agent. The data for the second crystal form (FpvA–Pvd–Ga) were collected on beamline BM30A at ESRF and the data set for the third crystal form (FpvA–Pvd–Fe) were collected on beamline BW7A at EMBL Hamburg. The data were processed using *XDS* (Kabsch, 1993) and scaled using *SCALA* (Evans, 1993) or *XDS*.

3. Results and discussion

Using FRET, an unknown fluorescent molecule was detected bound to the receptor after purification and could be a fluorescent Pvd precursor. It was easily removed by adding a large excess of Pvd–Fe and no fluorescence signal was observed after incubation of FpvA with Pvd–Fe owing to a total substitution of this fluorescent molecule by Pvd–Fe (Schalk *et al.*, 1999) (Fig. 1).

The first crystal form of FpvA–Pvd–Fe was obtained by mixing 15 mg ml^{−1} FpvA–Pvd–Fe with 12 mM MgSO₄, 12% PEG 3350 and 0.1 M sodium acetate pH 4.6. The second crystal form of FpvA–Pvd–Fe or FpvA–Pvd–Ga grew in a solution containing 5 mg ml^{−1} protein mixed with 7–10% PEG 4K, 0.1 M sodium citrate pH 5.6, 15% glucose, 10 mM CuSO₄ and 10% 2-propanol. The third crystal form was obtained by mixing 5 mg ml^{−1} FpvA–Pvd–Fe with 100–160 mM calcium acetate, 12% PEG 4K, 12% ethylene glycol and 0.1 M sodium cacodylate buffer pH 6.4. Crystals appeared quickly, reaching their maximum size after a few days, and their shape depended on the crystallization conditions since the same detergent was used in each case (Fig. 2). The resolution limits and quality of the diffraction data (Table 1) are quite variable depending on the crystal form.

The first form of the FpvA–Pvd–Fe crystals diffracted X-rays to 2.7 Å resolution. Systematic absences $00l$ for $l \neq 4n$ and $h00$ for $h \neq 2n$ resulted from the presence of screw axes. The crystal belongs to a tetragonal space group, with unit-cell parameters $a = 82.12$, $c = 286.23$ Å. This crystal form suffers rapidly from radiation damage on beamline ID29, but its high symmetry allowed the collection of a complete data set using one crystal. According to the Matthews coefficient calculation (Matthews, 1968), the solvent content is 56.2% and one molecule is in the asymmetric unit. Data for FpvA–Pvd–Ga were processed at 2.7 Å resolution, but the R_{sym} in the last resolution shell is higher than for the first crystal form. The crystal belongs to space group $C2$, with unit-cell parameters $a = 140.09$, $b = 235.03$, $c = 237.25$ Å, $\beta = 101.12^\circ$ and six molecules in the asymmetric unit. The solvent content is 66.9%, with a V_M of 3.71 Å³ Da^{−1}. Data from

the third crystal form of FpvA–Pvd–Fe were processed at 3.15 Å resolution. The crystal belongs to space group $C2$, with unit-cell parameters $a = 174.11$, $b = 123.13$, $c = 118.30$ Å, $\beta = 121.49^\circ$ and two molecules in the asymmetric unit. The solvent content is 60.9%.

The phase problem was solved by molecular replacement using *MOLREP* (Vagin & Teplyakov, 1997) from *CCP4* (Collaborative Computational Project, Number 4, 1994) using the SeMet–FpvA–Pvd

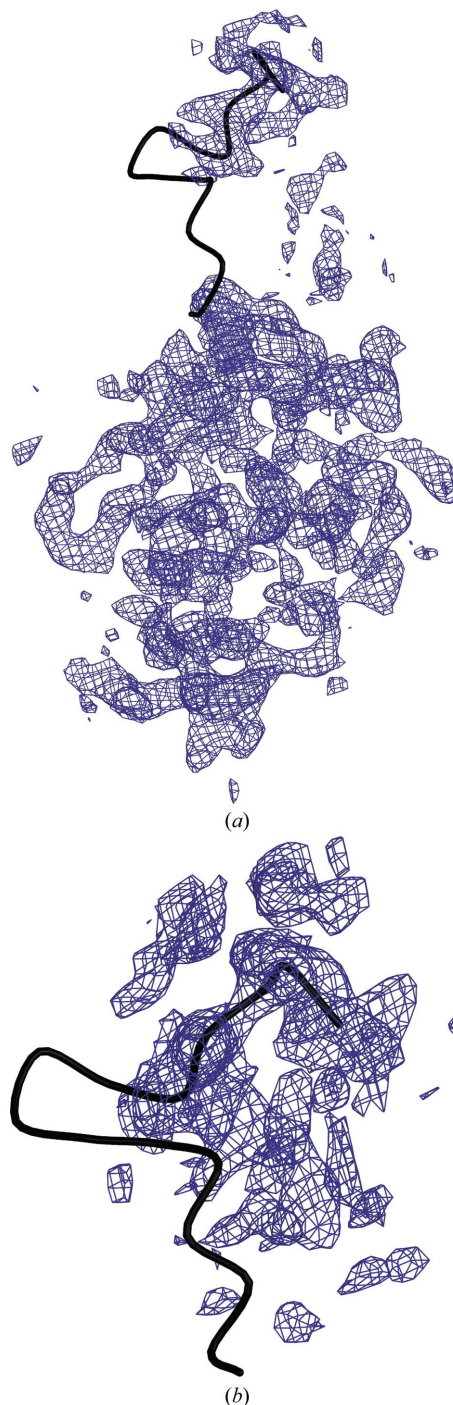


Figure 3

View of the N-terminal part of FpvA–Pvd (residues Ala129–Asp146) superimposed on a $3F_o - 2F_c$ electron-density map calculated for two space groups. (a) Space group $P4_12_12$: the map is calculated at 2.7 Å resolution and contoured at 1.2σ . Supplementary electron density corresponding to the signalling domain is observed. (b) Space group $C2$: the map is calculated at 2.7 Å resolution and contoured at 1.2σ .

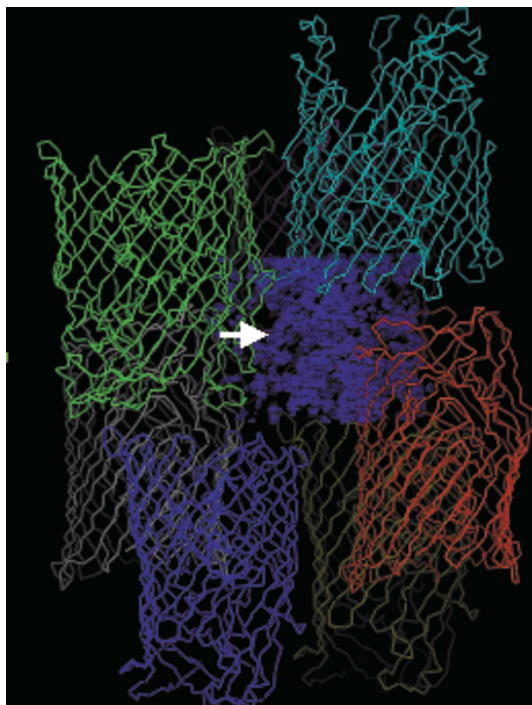


Figure 4

View of the crystal packing in space group $P4_12_12$ superposed on a $3F_o - 2F_c$ electron-density map. The electron density corresponding to the FpvA signalling domain is indicated by a white arrow.

(76 357 Da) atomic coordinates (PDB code 1xkh; Cobessi *et al.*, 2005) after replacing the Se atoms by S atoms. The space group for the first crystal form is $P4_12_12$. A $3F_o - 2F_c$ electron-density map was calculated after the molecular replacement for all the crystal forms and was superimposed on the FpvA–Pvd model. Analysis of the maps revealed that the electron density of the N-terminal part containing the signalling domain (10 130 Da) differed according to the crystal packing. Large connected peaks of electron density are only observed in the periplasmic part of FpvA–Pvd–Fe in space group $P4_12_12$ and are probably the signalling domain involved in the signal transduction (Figs. 3 and 4). Anomalous electron density is also observed where iron is expected.

Obtaining several crystal packings and working on several crystallization conditions have proved to be very useful in solving the structure of domains or disordered parts of a protein which could not be identified using one crystal form. Since the data collected from the first FpvA–Pvd–Fe crystal form are of better quality compared with the other data sets, model rebuilding at 2.7 Å resolution in space

group $P4_12_12$ is now under way. This analysis should provide structural details on the periplasmic signalling domain involved in the signal transduction as well as the structure of the Pvd–Fe conformer (Tzou *et al.*, 2005) bound to the binding site.

The authors would like to thank the staff of the BM30A beamline at ESRF and BW7A beamline at EMBL Hamburg for their kind assistance during the data collection as well the European Community Research Infrastructure Action under the FP6 ‘Structuring the European Research Area Programme’ contract No. RII3/CT/2004/5060008. We also thank Jason Greenwald for reading the manuscript. This work was supported by the Association Française de Lutte contre la Mucoviscidose (AFLM), by the ACI Interface Physique, Chimie, Biologie and the Dynamique et Réactivité des Assemblages Biologiques program from the Ministère de l’Enseignement Supérieur, de la Recherche et de la Technologie and the Centre National de la Recherche Scientifique.

References

- Braun, V., Mahren, S. & Ogierman, M. (2003). *Curr. Opin. Microbiol.* **6**, 173–180.
- Cobessi, D., Celia, H., Folschweiler, N., Schalk, I. J., Abdallah, M. A. & Pattus, F. (2005). *J. Mol. Biol.* **347**, 121–134.
- Collaborative Computational Project, Number 4 (1994). *Acta Cryst.* **D50**, 760–763.
- Cudney, R., Patel, S., Weisgraber, K., Newhouse, Y. & McPherson, A. (1994). *Acta Cryst.* **D50**, 414–423.
- Demange, P., Wendenbaum, S., Linget, C., Mertz, C., Cung, M. T., Dell, A. & Abdallah, M. A. (1990). *Biol. Met.* **3**, 155–170.
- Evans, P. R. (1993). *Proceedings of the CCP4 Study Weekend. Data Collection and Processing*, edited by L. Sawyer, N. Isaacs & S. Bailey, pp. 114–122. Warrington: Daresbury Laboratory.
- Ferguson, A. D. & Deisenhofer, J. (2002). *Biochim. Biophys. Acta*, **165**, 318–332.
- Ferguson, A. D. & Deisenhofer, J. (2004). *Cell*, **116**, 15–24.
- Garcia-Herrero, A. & Vogel, H. J. (2005). *Mol. Microbiol.* **58**, 1226–1237.
- Jancarik, J. & Kim, S.-H. (1991). *J. Appl. Cryst.* **24**, 409–411.
- Kabsch, W. (1993). *J. Appl. Cryst.* **26**, 795–800.
- Koebnik, R. (2005). *Trends Microbiol.* **13**, 343–347.
- Matthews, B. W. (1968). *J. Mol. Biol.* **33**, 491–497.
- Poole, K. & McKay, G. A. (2003). *Front. Biosci.* **8**, 661–686.
- Poole, K., Neshat, S., Krebes, K. & Heinrichs, D. E. (1993). *J. Bacteriol.* **175**, 4597–4604.
- Schalk, I. J., Kyslik, P., Prome, D., Van Dorsselaer, A., Poole, K., Abdallah, M. A. & Pattus, F. (1999). *Biochemistry*, **38**, 9357–9365.
- Schalk, I. J., Yue, W. W. & Buchanan, S. K. (2004). *Mol. Microbiol.* **54**, 14–22.
- Tzou, D. L., Wasielewski, E., Abdallah, M. A., Kieffer, B. & Atkinson, R. A. (2005). *Biopolymers*, **79**, 139–149.
- Vagin, A. & Teplyakov, A. (1997). *J. Appl. Cryst.* **30**, 1022–1025.
- Yue, W. W., Grizot, S. & Buchanan, S. K. (2003). *J. Mol. Biol.* **332**, 353–368.